Omni-Akuatika, 19 (1): 69 - 81, 2023
ISSN: 1858-3873 print / 2476-9347 online

Research Article

journal homepage: http://ojs.omniakuatika.net

The Impact of MJO-C and MJO-B Upon Sea Surface Temperature and Rainfall in Indonesia

Lalu Mantigi Wana Paksi[1*], Simon Tubalawony[2], Harold Joppie Davido Waas[2], Karisma R. Muthmainnah[3]

[1] *Marine Science Postgraduate Program, Pattimura University, Indonesia*
[2] *Marine Science Study Program, FPIK, Pattimura University*
[3] *BPS – Statistics Indonesia, Indonesia*

**Corresponding author: lalu.paksi@bmkg.go.id*

Received 1 January 2023; Accepted 5 July 2023; Available 18 July 2023

ABSTRACT

Madden Julian Oscillation (MJO) based on its propagation through the maritime continent can be divided into two types, namely MJO-C (Crossing) and MJO-B (Blocked) as evidenced by the spatial diagram of Hovmöller OLR anomaly. This study aimed to determine the effect of MJO variations, namely MJO-C and MJO-B on sea surface temperature and rainfall in the Indonesian region in the period of 1998 to 2015. The data used in this study are reanalysis models including sea surface temperature and rainfall with composite events (one month before propagation, during propagation, and one month after propagation of MJO-C and MJO-B). The results show that when MJO-C and MJO-B are active, sea surface temperature and the amount of rainfall are increased, especially in equatorial Indonesia and the southern hemisphere. When compared, MJO-C has a more significant impact than MJO-B.

Keywords: MJO, Sea Surface Temperature, Precipitation

ABSTRAK

Madden Julian Oscillation (MJO) berdasarkan propagasinya melewati benua maritim dapat dibagi menjadi dua jenis yaitu MJO-C (Crossing) dan MJO-B (Blocked) yang dibuktikan dengan spasial diagram Hovmöller anomali OLR. Penelitian ini bertujuan untuk mengetahui pengaruh dari variasi MJO, yakni MJO-C dan MJO-B terhadap arah dan kecepatan angin, suhu permukaan laut dan curah hujan di wilayah Indonesia pada periode tahun 1998 hingga 2015. Data yang digunakan dalam penelitian ini adalah model reanalysis meliputi data suhu permukaan laut, dan curah hujan dengan komposit kejadian (satu bulan sebelum propagasi, saat propagasi, dan satu bulan setelah propagasi MJO-C serta MJO-B). Hasil penelitian menunjukkan bahwa saat MJO-C dan MJO-B aktif berdampak terhadap peningkatan suhu permukaan laut serta peningkatkan jumlah curah hujan khususnya di wilayah Indonesia bagian ekuator dan belahan bumi selatan (BBS). Jika dibandingkan, MJO-C memiliki dampak yang lebih signifikan dibandingkan MJO-B.

Kata kunci: MJO, Suhu Permukaan Laut, Presipitasi

1. Introduction

The Madden Julian Oscillation (MJO) is an intraseasonal wave or oscillation that occurs in the troposphere of the tropics, from the Indian Ocean to the Central Pacific, traveling from west to east. MJO can cause the interaction between the atmosphere and the ocean, resulting in fluctuations in tropical sea surface temperature (SST) and rainfall (Madden and Julian, 1972). Zhang and Ling (2017) classify MJO into two subtypes, MJO-C (crossing) and MJO-B, based on propagation patterns in the Maritime Continent region (blocked). MJO-C is a MJO that survived and traversed the "Crossing" of the Maritime Continent, whereas MJO-B endured "Blocking" or was blocked by the Maritime Continent. In this research, it was determined that the MJO underwent amplitude attenuation as it approached the Maritime Continent, where the propagation abilities of MJO-B and MJO-C differed in the 100̊ East area. MJO-C is able to sustain its amplitude after passing 100̊ E, but MJO-B is unable to do so and hence weakens and vanishes (barrier effect).

Observing the MJO-C and MJO-B propagation using outgoing longwave radiation is

http://dx.doi.org/10.20884/1.oa.2023.19.1.1057

one method (OLR). Outgoing Longwave Radiation is the term for longwave energy that enters certain levels of the atmosphere (OLR). The OLR value indicates the highest temperature and humidity of the atmosphere. The utilized number reflects the amount of convective activity that can limit the earth's radiation emission. Negative (positive) OLR readings indicate a rise (down) in the area's convection activity (Hidayat and Kizu*, 2010*). OLR factors are also influenced by Sea Surface Temperature (SST) and Rainfall (Hidayat and Kizu, 2010; Balbeid et al., 2015).

Research related to the correlation between MJO and sea surface temperature, earlier conducted by Haryanto, et al., (2022) resulted in an increase in sea surface temperature when the MJO was active. Changes in sea surface temperature influence the variability of rainfall, and it is believed that this is due to the interaction between the atmosphere and the sea, which involves the spatial and temporal movement of water masses. According to several research findings, Indonesian rainfall events and the SST phenomena are clearly related (Nuryanto and Badriya, 2014). On the other hand, Arbain et al., (2017) categorized the effect of MJO on rain with a composite of events before, after and when the MJO is active and the results showed that the distribution of the maximum increase in rain occurred at the time before the active MJO.

With the variation of MJO, especially MJO-C and MJO-B, the response of the atmosphere and ocean interaction is also expected to be different. Therefore, this study determined MJO variations and their impact on sea surface temperature, and rainfall in the Indonesian region with a composite of events before, after and when MJO-C and MJO-B had been active.

2. Materials and methods

Research Location

The research site that is the focus of this research is located in Indonesia with coordinates (12°N to 12°S and from 90°E to 145°E). From 1998 to 2015, a seventeen-year time frame was utilized for this research with a composite event (one month before propagation, during propagation, and one month after propagation of MJO-C and MJO-B).

Research Data

This research utilizes MJO-B and MJO-C event data, OLR data, sea surface temperature, and rainfall data:

a) Kerns and Chen's 2016 research yielded information regarding MJO-B and MJO-C occurrences. The 16-year span for the MJO-B and MJO-C event data runs from 1998 to 2015 (Table 1 and Table 2).
b) Data on the composite of events' sea surface temperature (SST) for the years 1998 to 2015 (one month before propagation, during propagation, and one month after MJO-C and MJO-B propagation). The data is available online on the Copernicus website (https://data.marine.copernicus.eu/) in .nc format. The data comes from a reanalysis model and has a temporal resolution of one hour and a spatial resolution of 0.05° × 0.05°.
c) Rainfall precipitation data for the period 1998-2015 for the composite events (one month before propagation, during propagation, and one month after MJO-C and MJO-B propagation). The data was obtained from the website of The Tropical Rainfall Measuring Mission (TRMM) NASA Global Precipitation Measurement Mission (https://gpm.nasa.gov/missions/trmm) in .nc format. Spatial data resolution 0.25° × 0.25° with 1 hour temporal resolution.

Table 1. Table of Event Time Duration, and Velocity of MJO-C (Kerns and Chen, 2016)

No.	Event Time	Duration (Days)	Speed (m/s)	No.	Event Time	Duration (Days)	Speed (m/s)
1.	17/09/1998	17.9	3.5	**14.**	02/12/2007	59.2	2.5
2.	15/01/1999	29.8	3.9	**15.**	17/01/2008	35.4	3.4
3.	23/11/1999	26.9	4.6	**16.**	29/09/2008	33.2	2.5
4.	07/11/2000	31.2	4.0	**17.**	20/12/2008	18.4	2.3
5.	15/12/2000	16.1	6.4	**18.**	11/11/2009	17.0	4.6
6	04/1/2002	61.0	2.4	**19.**	15/11/2011	25.4	4.7
7.	11/12/2002	32.9	5.3	**20.**	12/12/2011	27.0	4.2
8.	21/09/2003	29.5	2.5	**21.**	18/02/2012	42.8	3.0
9.	23/11/2003	47.8	2.4	**22.**	11/12/2012	43.4	0.4
10.	18/01/2004	30.4	5.8	**23.**	22/12/2013	40.9	2.8
11.	17/09/2004	20.8	4.2	**24.**	15/11/2014	24.5	3.0
12.	17/02/2006	31.9	3.9	**25.**	13/12/2014	39.8	1.6
13.	12/12/2006	39.9	4.5				

Table 1 explains Kerns and Chen's 2016 research yielded information regarding MJO-C occurrences. The 16-year span for the MJO-C event data runs from 1998 to 2015.

Table 2. Table of Event Time, Duration, and Velocity of MJO-B (Kerns and Chen, 2016)

No.	Event Time	Duration (Days)	Speed (m/s)	No.	Event Time	Duration (Days)	Speed (m/s)
1.	26/12/1999	15.00	5.6	9.	05/01/2009	13.38	3.7
2.	13/02/2000	11.50	3.5	10.	21/01/2009	13.25	6.0
3.	28/01/2001	35.25	2.4	11.	18/10/2011	18.50	3.7
4.	28/11/2001	27.00	3.0	12.	20/10/2012	14.88	3.2
5.	21/01/2003	14.88	3.4	13.	01/11/2012	13.75	3.0
6	14/02/2003	11.75	4.6	14.	22/12/2012	7.12	4.8
7.	13/01/2007	10.50	6.3	15	06/11/2013	15.25	2.7
8.	26/02/2008	8.62	3.6	16.	11/10/2014	9.88	3.6

Table 2. explains Kerns and Chen's 2016 research yielded information regarding MJO-B occurrences. The 16-year span for the MJO-B event data runs from 1998 to 2015.

Data Analysis Procedures

MJO-B and MJO-C events were chosen according to research by Kerns and Chen (2016). Then, the events were modified into a composite of the events described in Arbain (2017), namely one month before, during, and one month after MJO-C and MJO-B propagation. Then, OLR data, sea surface temperature, and rainfall were filtered according to the composite period of MJO-C and MJO-B. The data was then analyzed visually in the form of a map for each dataset (Bukhari et al., 2017). In addition, the propagation of MJO-C and MJO-B was analyzed using filtered OLR anomaly data and Hovmöller diagram analysis in accordance with study (*Hidayat & Kizu, 2010*).

Chart Analysis *Hovmöller*

The *Hovmöller* diagram was used to determine the propagation of MJO-C and MJO-B using an analytical method. This study used OLR anomalies in the form of Hovmöller diagrams to identify the strengthening or weakening of the ongoing MJO-C and MJO-B propagation with latitude limits of 5°N - 5°S and longitude limits of 80°W - 180°E (Jones et al., 1998; Hendon et al., (2007).

Temporal and Spatial Analysis

The temporal and geographical analysis seeks to determine the spatial and temporal variations in OLR anomaly, sea surface temperature, and precipitation. Based on the composite of MJO-C and MJO-B occurrences, the temporal analysis seeks to determine the quantity of precipitation, OLR anomaly, average wind direction and speed, and average sea surface temperature from daily data. The objective of spatial analysis was to characterize changes in the distribution of precipitation, OLR anomalies, average wind direction and speed, and average sea surface temperature in the studied region.

Quantitative Comparative Analysis

Sea surface temperature and rainfall data are displayed in the form of maps of average sea surface temperature and rainfall amounts during the composite of MJO-B and MJO-C events using the GrADS application. Then an analytical descriptive analysis of the resulting map results was carried out, to determine the effect of the relationship between MJO-C and MJO-B events and their impact on sea surface temperature and rainfall in the research region.

3. Results and Discussion

MJO Propagation over the Indonesian Sea

The propagation of the Madden Jullian Oscillation in the Indonesian Sea is indicated by a significant decrease in the value of longwave radiation (OLR) emitted by the earth's surface and an increase in zonal wind speeds at various altitudes from sea level to the tropopause along the equator. The decrease in OLR value is caused by wave obstacles communicated to the atmosphere, one of which is the creation or expansion of cumulus clouds (rain clouds) in the Indian Ocean, also known as super cloud clusters (SCCs). A negative OLR anomaly value might imply a drop in the OLR value. OLR characteristics can indicate convection activity, hence MJO propagation can be seen in Indonesia.

One of the methods to analyze and observe the propagation of MJO is using Outgoing Longwave Radiation (OLR) data. Longwave radiation that reaches a certain layer of the atmosphere is called Outgoing Longwave Radiation (OLR). The OLR value represents the peak temperature and water vapor content of the atmosphere. OLR is a meteorological parameter that can be used to observe the Madden Jullian Oscillation (MJO) phenomenon.

The correlation between OLR and MJO is evident in the variation of OLR measured from satellite infrared sensors. The MJO phenomenon is related to the formation of warm pools in the eastern Indian Ocean and the western Pacific Ocean so that the movement of MJO to the east along with the westerly wind along the equator is always followed by thick cumulus cloud convection (Evana et al., 2008). MJO is characterized by convective clouds so that if the OLR value is positive, the convective clouds are low. Meanwhile, a negative OLR value indicates that the productivity of convective clouds in the area is high (Permana, 2014).

OLR Anomaly Hovmoller Analysis of MJO-C Propagation

The OLR anomaly research is shown in the form of a Hovmöller diagram, which serves to illustrate the propagation of MJO in Indonesia on a temporal and regional scale (Figure 1 (a)). The analysis was conducted across a limited range, from 5° South Latitude to 5° South Latitude. This is done to produce a significant MJO signal, as Jones et al., (1998) and Hendon et al., (2001) did (2007).

Positive OLR anomaly patterns are observed in the majority of Indonesia (Figure 1 (a)). With the highest OLR Anomaly value between 12 November and 12 December 2016 being between 60 and 90 W/m^2. The negative anomaly shifted from west to east between November 1 and November 23, 2016, with a maximum value of 90 W/m^2. A negative (positive) OLR anomaly indicates a rise (decrease) in convection activity within an area (Hidayat & Kizu, 2010). Consequently, there is no major convective activity in Indonesia (Figure 1 (a)).

Zhang and Ling (2017) classifies MJO based on the pattern of the kind of propagation while in the region of the Maritime Continent, namely MJO-B (blocked), MJO experiencing "*Blocking*" or being blocked by the maritime continent, and MJO-C "*Crossing*." A negative OLR anomaly that retains its magnitude after passing 100° East indicates the propagation of the MJO-C. Negative anomaly values first appeared between 12 December 2006 and 22 January 2007 are shown in the dash-dotted black box. (Figure 1 (b)).

This negative OLR anomaly expands to the east, with lesser values ranging from -90 to -70 W/m^2 on a larger scale (Figure 1 (b)). A negative (positive) OLR anomaly indicates a rise (decrease) in convection activity within an area (Hidayat & Kizu, 2010). Thus, tremendous convective activity exists in the Indonesian area.

One month following the activation of MJO-C, anomalous circumstances exhibited a positive OLR anomaly pattern throughout the majority of Indonesia ranging from -90 to 90 W/m^2 on January 23 to February 23, 2007 indicated by the dash-dotted red box. This positive anomaly with the greatest value of 90 W/m^2 goes from west to east (Figure 1 (c)). A positive OLR anomaly indicates a decrease in convection in the area (*Hidayat & Kizu, 2010*). This indicates a lack of major convective activity throughout a large portion of Indonesia (Figure 1 (c)).

OLR Anomaly Hovmoller Analysis of MJO-B Propagation

Zhang and Ling (2017) categorize MJO based on the kind of propagation pattern while in the region of the Maritime Continent: MJO-B (blocked) is MJO that experiences "*Blocking*" or is blocked by the maritime continent, and MJO-C "*Crossing*" is MJO that crosses the maritime continent. MJO-B was unable to sustain its amplitude, hence it was unable to pass 100° East and eventually dissipated.

A negative OLR anomaly pattern is seen one month before an active MJO-B. From September 21 to October 6, this negative anomaly spreads from east to west are shown in the dash-dotted black box (Figure 2 (a)). A

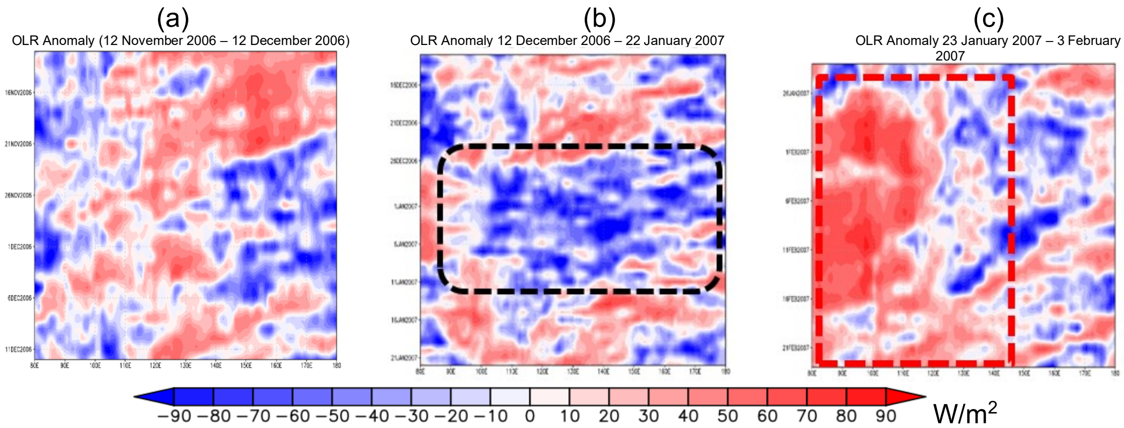

Figure 1. OLR Anomaly Before MJO-C is Active (a), OLR Anomaly When MJO-C is Active (b), OLR Anomaly After MJO-C is Active (c)

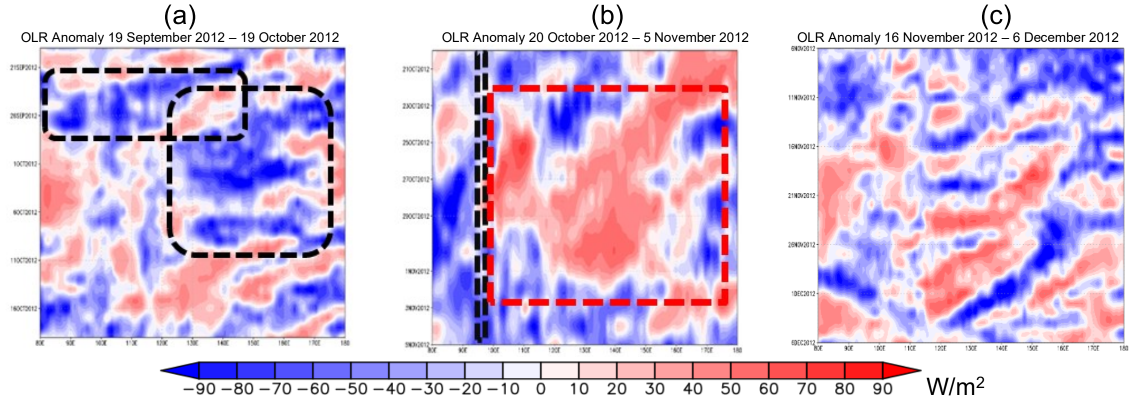

Figure 2. OLR Anomaly Before MJO-B is Active (a), OLR Anomaly When MJO-B is Active (b), OLR Anomaly After MJO-B is Active (c)

small proportion of the islands of Papua, Maluku, Sulawesi, and Sumatra are uniformly dispersed with negative OLR anomaly values ranging from -70 to -90 W/m^2. Negative OLR anomalies might boost regional convection activity (Hidayat & Kizu, 2010). Consequently, reflecting convective activity in the area of Indonesia (Figure 2 (b)).

The MJO-B signal cannot sustain its amplitude, therefore it is unable to reach 100° East and gradually loses strength until it evaporates. It is evident that the MJO propagation is diminishing, since it no longer reaches 100º East shown in discontinuous black and red boxes (Figure 2 (b)). In addition, the majority of OLR anomalies during the MJO-B phase are in a positive state. This may occur as a result of the effect of MJO activity and their progressive diminishing in western Indonesia. The dominance of this positive anomaly might diminish convective activity that connects the atmosphere to the sea (Figure 2 (b)).

After one month of MJO-B activity, a negative OLR anomaly pattern emerged. From November 6 to December 6, 2012, this negative anomaly shifts from west to east (Figure 2 (c)). The negative OLR anomaly values range from -70 to -90 W/m^2 and are uniformly distributed from Sumatra to Papua. Negative OLR anomalies might boost regional convection activity (*Hidayat & Kizu, 2010*). This indicates the presence of convective activity on Indonesian land, which might enhance the interaction between the atmosphere and the ocean (Figure 2 (c)).

MJO Variation Propagation Results Using OLR Anomalies

Based on the results of the research that has been carried out in this study, the intensity of MJO-C is high and is able to maintain its amplitude after crossing 100˚ east which is characterized by OLR intensity. OLR anomalies that occur during active MJO-C have negative anomaly values compared to the time span of one month after and before the occurrence of MJO-C. The high negative OLR anomaly that occurs in the research area is due to the large amount of convective cloud cover that receives and reflects longwave radiation from the earth. Because negative (positive) OLR anomalies represent an increase (decrease) of convection activity in the region (Hidayat and Kizu, 2010).

Then the propagation of MJO-B (Figure 2 (b)), MJO-B could not maintain its amplitude, so it could not cross 100o east and experienced weakening until it disappeared. There is a clear weakening of MJO propagation that does not reach 100° east. When MJO-B is active, convective activity increases in the western Indian Ocean, absorbing the surrounding air mass. This causes reduced convective activity in Indonesia, which is characterized by positive OLR anomalies in a number of regions (Figure 2 (b)).

Impact of MJO on Sea Surface Temperature

The dynamics and variability of sea surface temperature (SST) in the equatorial region, especially in the Indonesian Maritime Continent during the active phase of the MJO, is affected by the influx and discharge of latent heat from the land-sea-atmosphere system. Wirasatriya et al., (2018) explained that low SPL is caused by increasing wind speed, and vice versa. Areas with strong wind speeds, latent heat release is also high. Latent heat flux has an important role in adjusting the heat dissipation that was driven by wind speed.

Asymmetric heating of the ocean surface results in variations that affect sea surface temperature (SST) on an intraseasonal scale. Diurnal SST variations have the effect of increasing SST variations on the intraseasonal scale. By observing the influence of sea surface temperature on the intraseasonal scale, it can be concluded that diurnal SPL variations play a role in MJO convection. In another study, it was stated that diurnal variability of SST can increase the strength and coherence of the MJO through the process of ocean-atmosphere coupling on a time scale of 20-100 days (Seo et al., 2014).

Interaction of Sea Surface Temperature with MJO-C

One of the dynamics and variability of sea surface temperature (SST) in the equatorial area, particularly in the Indonesian Maritime Continent during the active phase of the MJO, is impacted by the system of input and release of latent land-sea-atmosphere heat. According to Wirasatriya et al., (2018), the low SST was caused by an increase in wind speed, and vice versa. In regions with high wind speeds, latent heat release is likewise high. The significance of latent heat flux in controlling heat release, which is regulated by wind speed, is crucial.

Asymmetric warming of the ocean surface results in variations that affect sea surface temperature (SST) on an intra-seasonal scale. Diurnal SST variations have the effect of magnifying SST variations on the intramuscular scale. By observing the affects of sea surface temperature on the intra-seasonal scale, it can be concluded that diurnal SST variations play a role in MJO convection. In another study, it was stated that diurnal SST variability can increase the strength and coherence of the MJO through the process of ocean-atmosphere coupling on a time scale of 20-100 days (Seo et al., 2014).

One month before to the propagation of MJO-C (12 November - 12 December 2006), sea surface temperature analysis revealed that the lowest temperature was between 25 ^{0}C and 27 ^{0}C in the area of Sumatra Island south of the seas of Java Island (Figure 3 (a)). In contrast, the northern seas of Java and Sumatra Island are warmer, ranging between 29 ^{0}C and 31 ^{0}C.

The spatial distribution of sea surface temperature from 12 November to 12 December 2006 indicates that the average sea surface temperature ranges from around 25 ^{0}C to 31 ^{0}C, with only a few coastal regions of Sumatra and Java having sea surface temperatures below 27 ^{0}C. The waters of Sulawesi, Bali-Nusa Tenggara, Kalimantan, North Maluku, and Papua have the greatest average sea surface temperature of 30 ^{0}C to 31 ^{0}C, while the seas of Java, Sumatra, and the Sea have the lowest average sea surface temperature 25.5 ^{0}C to 27.5 ^{0}C is the average sea surface temperature in the Arafura.

The depiction of the spatial distribution of the average sea surface temperature during active MJO-C in Indonesian waters from 12 November to 22 January 2007 (Figure 3 (b)). The range of sea surface temperatures in coastal regions, such as the southern portion of Sumatra and Java seas, is between 27 ^{0}C and 30 ^{0}C, and the average sea surface temperature is higher than it was during the last event. While the seas of Nusa Tenggara, Sulawesi, Kalimantan, Maluku, and Papua have an average warmest sea surface temperature of 31 ^{0}C, with a range of 29.5 ^{0}C to 31 ^{0}C.

After the January 23 to February 23, 2007 propagation of MJO-C, the regional distribution of mean sea surface temperatures varied from 25 ^{0}C to 31 ^{0}C (Figure 3 (c)). In the seas between the western portion of Kalimantan Island and the eastern portion of Sumatra Island, the sea surface temperature ranges from 25 ^{0}C to 27 ^{0}C. Meanwhile, the warmest average sea surface temperature occurs between 30 ^{0}C and 31 ^{0}C in the seas of Sulawesi, Nusa Tenggara, and Kalimantan. This analysis demonstrates that the average sea surface temperature is declining in a number of places, including the seas of Sulawesi, Nusa Tenggara, Maluku, and Papua.

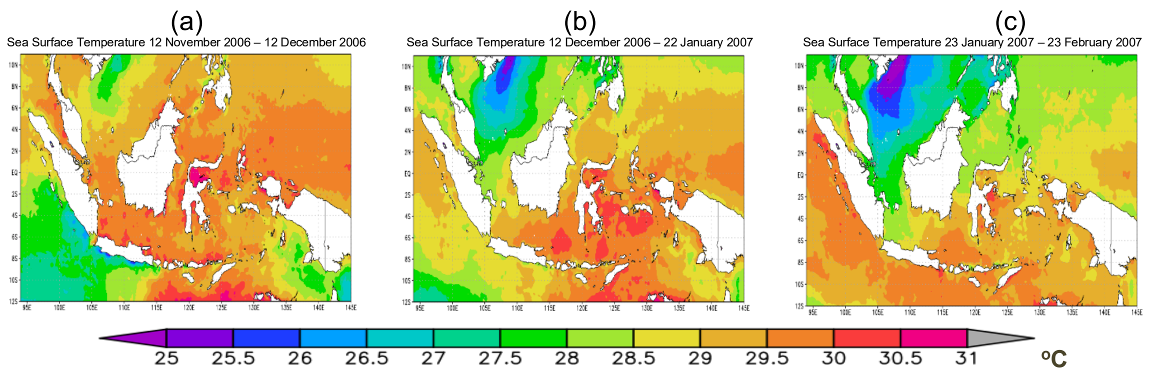

Figure 3. Average Sea Surface Temperature Before Active MJO-C (a), Average Surface Temperature During Active MJO-C (b), Average Surface Temperature After Active MJO-C (c)

Interaction of Sea Surface Temperature with MJO-B

One of the dynamics and variability of sea surface temperature (SST) in the equatorial area, particularly in the Indonesian Maritime Continent during the active phase of the MJO, is controlled by the system of heat exchange between land, sea, and atmosphere. One month before to the MJO-B propagation from September 19 to October 19, 2012, the area of Sumatra Island to the south of the waters of Java Island, Bali, Nusa Tenggara, Maluku, and Papua had the lowest sea surface temperature of 25 °C to 27 °C, according to an examination of sea surface temperature. The northern seas of Java and Sumatra Island are warmer, ranging from 29 ^{0}C to 30 ^{0}C (Figure 4 (a)).

The waters of northern Sulawesi, Kalimantan, and North Maluku have the highest average sea surface temperature at 30 ^{0}C to 31 ^{0}C, while the waters of southern Sumatra, Java, Bali, Nusa Tenggara, Maluku, and Papua have the lowest average sea surface temperature at 25 ^{0}C to 27.5 ^{0}C.

The regional distribution of the average surface temperature of the Indonesian Maritime Continent Sea, which ranged from 25 ^{0}C to 31 ^{0}C when MJO-B was active from October 20 to November 5, 2012, is depicted in this picture. Compared to sea surface temperatures before MJO-B was active, the average sea surface temperature has mostly risen and gotten higher in numerous ocean regions (Figure 4 (b)). The seas of Nusa Tenggara, Sulawesi, Kalimantan, Maluku, and Papua have an average warmest sea surface temperature of 31 ^{0}C, with a range of 29.5 ^{0}C to 31 ^{0}C.

In the southern seas of Sumatra, Java, Bali, Nusa Tenggara, Arafura Sea, and Papua, the temperature ranges from 25 ^{0}C to 27.5 ^{0}C. In comparison, the seas to the north of Nusa Tenggara, Bali, Java, and Sumatra Island are between 29 ^{0}C and 30.5 ^{0}C warmer. Iillustrated that the seas of northern Sulawesi, Kalimantan, and north Maluku have the highest average sea surface temperature, ranging from 30 ^{0}C to 31 ^{0}C (Figure 4(b)).

The regional distribution of the average surface temperature of the Indonesian Maritime Continent Sea one month after MJO-B began active from November 6 to December 6, 2012, with temperatures ranging from 25 ^{0}C to 31 ^{0}C (Figure 4 (c)). In numerous water regions, the majority of the average sea surface temperature has climbed to become warmer than when MJO-B is active. The seas of Nusa Tenggara, Sulawesi, Kalimantan, Maluku, and Papua have a sea surface temperature range between 29.5 ^{0}C and 31 ^{0}C, with an average warmest sea surface temperature of 31 ^{0}C.

In the southern seas of Sumatra and Java, temperatures range from 25 ^{0}C to 27.5 ^{0}C. In comparison, the seas to the north of Nusa Tenggara, Bali, Java, and Sumatra Island are between 29^{0}C and 30.5 ^{0}C warmer. The seas of Sulawesi, Kalimantan, Maluku, and North Maluku have the highest average sea surface temperature, which ranges from 30 ^{0}C to 31 ^{0}C (Figure 4 (c)).

Results of the Effect of MJO Variations with Sea Surface Temperature

Several mechanisms including evaporation, cloud formation, local wind impacts, and variations in inter- and intra-hemisphere heat transport might influence the Sea Surface Temperature Variability. Changes in the fluctuation of latent heat loss from the sea surface are a key factor in sea surface temperature variations. Other variables that can influence the sea surface temperature include currents, waves, convection, upwelling, divergence, and the freezing and melting of polar ice.

When MJO-C is active, areas of Sumatra, Kalimantan, and the central and northern portions of Sulawesi Island have negative OLR

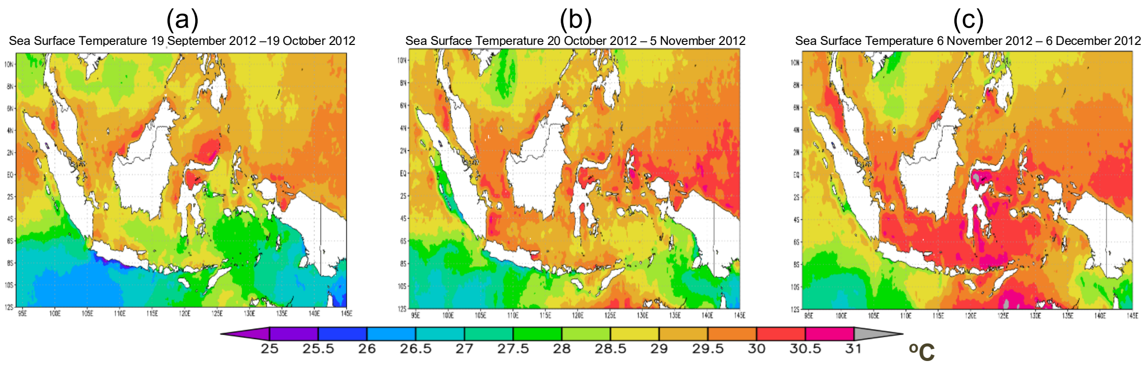

Figure 4. Average Sea Surface Temperature Before Active MJO-B (a), Average Surface Temperature During Active MJO-B (b), Average Surface Temperature After Active MJO-B (c)

anomalies. Then go towards the Maluku Islands and West Papua in the east. In addition, the negative OLR anomaly moves towards the northern portion of Papua Island towards the east. Haryanto (2021) indicated, based on earlier research, that when MJO propagation penetrates the Maritime Continent region, it might cause a rise in the surrounding sea surface temperature (Kim et al., 2017). In contrast to MJO-B, which cannot approach the Maritime Continent (Indonesian territory) because it cannot sustain its amplitude, so it cannot cross 100̊ E before weakening and dissipating, the PDO may penetrate the Maritime Continent (Barrier Effect).

When the active MJO-C phase may enhance sea surface temperatures, the propagation of MJO through the tropics is an occurrence of ocean-atmospheric interaction, according to the result of this research (Figure 5). This interaction can alter the physical attributes of the sea and atmosphere; one example is the greater sea surface temperature in the southern section of the Maritime Continent (the eastern part of the Indian Ocean south of Java, the Banda Sea, and the Timor Sea) during MJO-C compared to MJO-B (Figure 6).

According to Abdullah's (2018) research, the MJO has the ability to cause variations in sea surface temperature (especially in the Equator region). Due to an increase in evaporation and cloud formation during the active period of the MJO, the SST value rises. During the active period of MJO, Baeda et al., (2019) discovered that MJO had a significant influence on variations in SST values, with an 80.2% correlation.

The Effect of MJO on Rainfall

The region of Indonesia has complex atmospheric dynamics that contribute to the variability of rainfall. Rainfall variations in Indonesia are affected by global, regional, and local scale phenomena, on various time scales such as the Asian and Australian monsoons, ENSO, and the Madden Julian Oscillation. Convective impacts in the atmosphere significantly affect the process of convective cloud development and the amount of rainfall produced (Prayuda and Alfuadi, 2015). The occurrence of a significant quantity of convective clouds on a large scale is known as Super Cloud Clusters (SCCs), which indicates the activity of the MJO and can affect rainfall in the Indonesian region (Arbain et al., 2017).

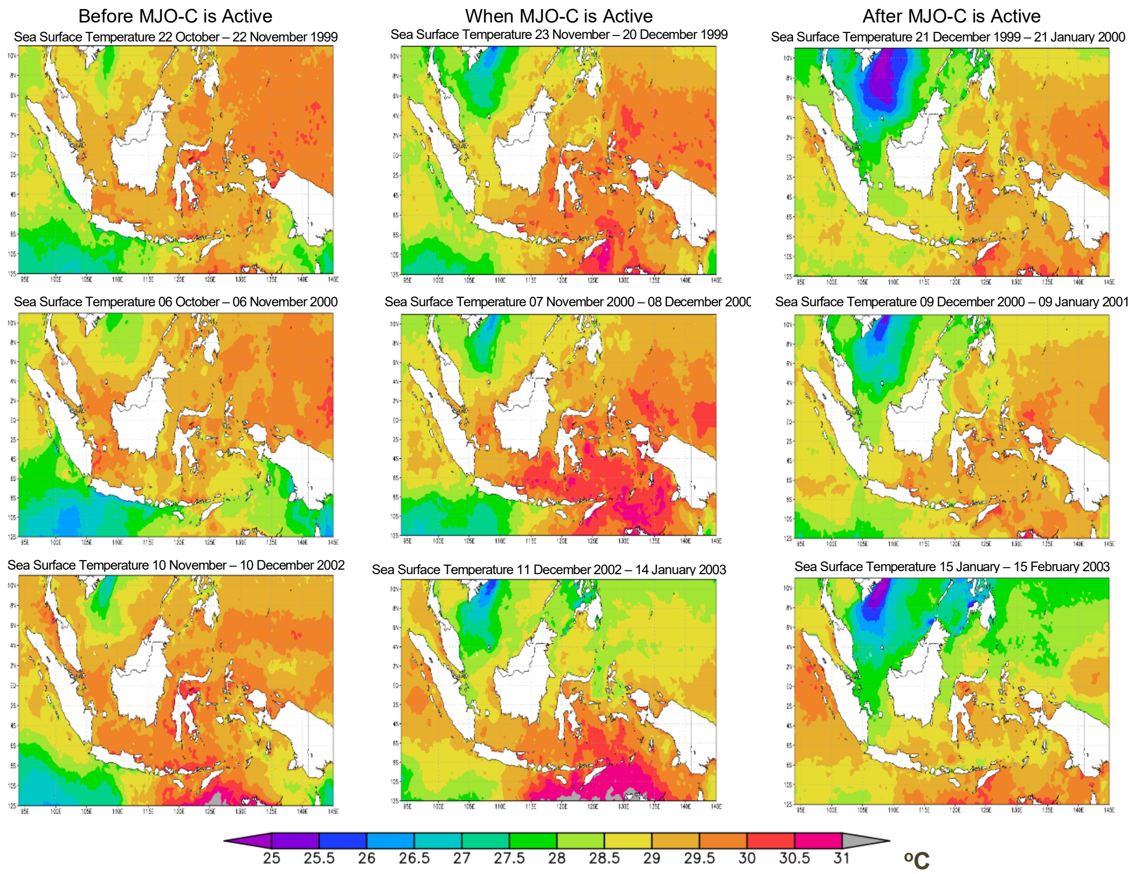

Figure 5. Response of Average Sea Surface Temperature to the MJO-C Composite (°C)

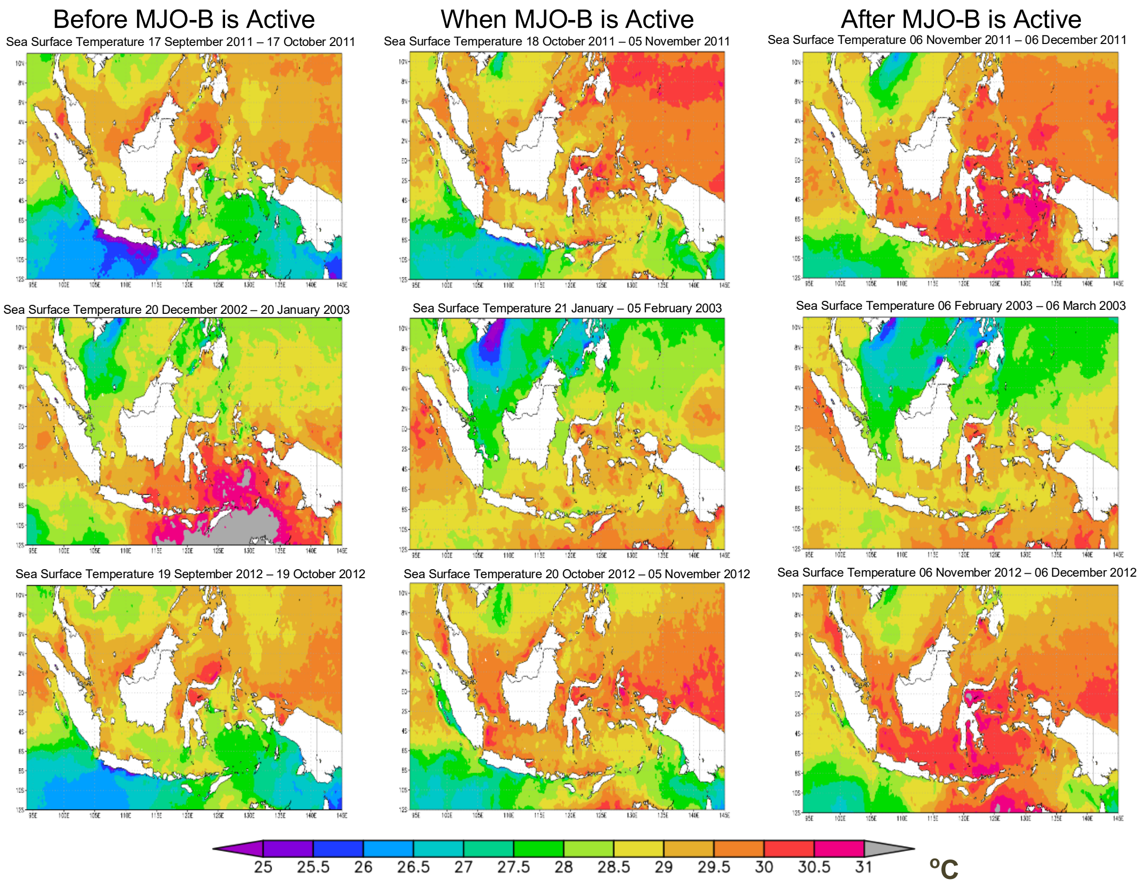

Figure 6. Response of Average Sea Surface Temperature to the MJO-B Composite (°C)

Interaction of Total Rainfall with MJO-C

One month before to the MJO-C propagation from 12 November to 12 December 2006, the analysis of daily rainfall in Indonesia revealed a range of 0 mm to 700 mm. In the Indian Ocean region, the western part of Sumatra, the islands of Sumatra, Java, and Kalimantan receive the most rainfall, which ranges from 0 to 700 mm. The distribution of rainfall with low values in the areas of Bali, Nusa Tenggara, Maluku, Sulawesi, and Papua, with values ranging from 0 mm to 300 mm (Figure 7 (a)).

When the MJO-C occurred from 12 December 2006 to 22 January 2007, the geographical distribution of the quantity of rainfall in the majority of Indonesian regions that received an increase in rainfall from the event before the MJO-C was active ranged from 0 mm to 1300 mm (Figure 7 (b)). The regions of Kalimantan, Sumatra, Java, and parts of the Java Sea, Bali Sea, and Makassar Sea receive between 900 and 1300 millimeters of rainfall on

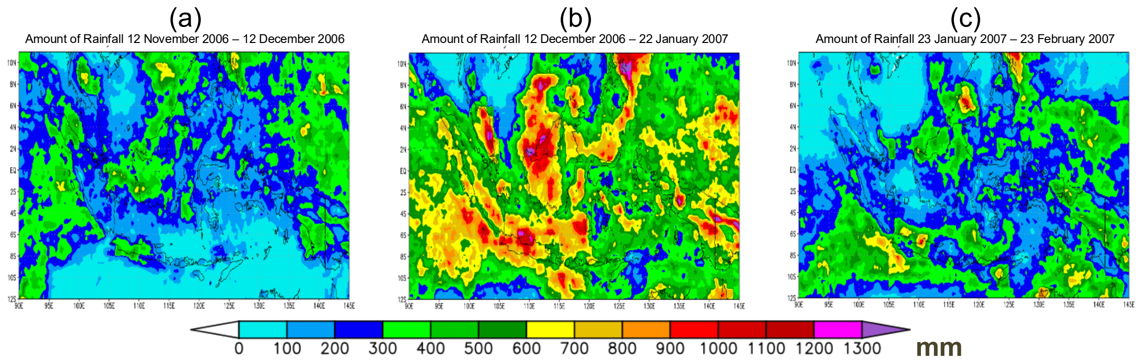

Figure 7. Amount of Rainfall Before MJO-C is Active (a), Amount of Rainfall When MJO-C is Active (b), Amount of Rainfall After MJO-C is Active (c)

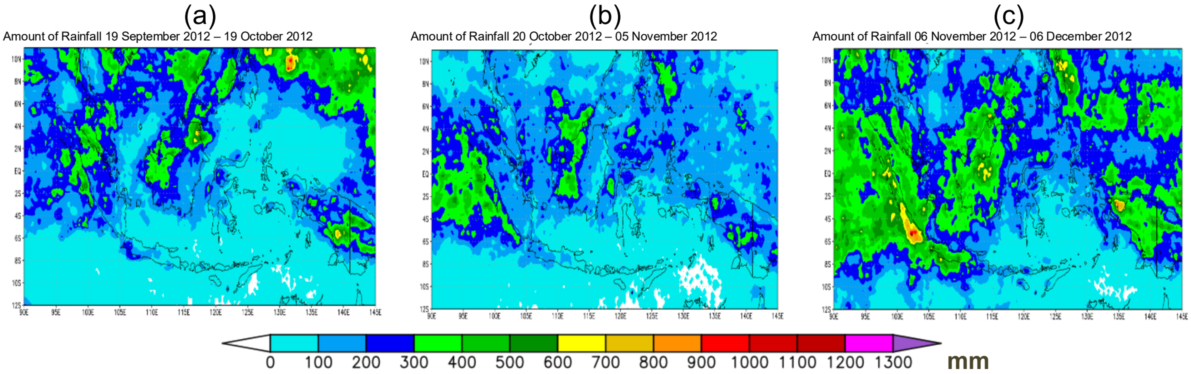

Figure 8. The Amount of Rainfall Before MJO-B is Active (a), Amount of Rainfall When MJO-B is Active (b), Amount of Rainfall After MJO-B is Active (c)

average. The regions of Nusa Tenggara, Maluku, North Maluku, and parts of Papua receive the least amount of rainfall, with values ranging from 0 mm to 500 mm.

One month after the propagation of MJO-C from January 23 to February 23, 2007, the amount of daily rainfall with the analysis revealed that the majority of regions in Indonesia experienced a decrease in rainfall compared to the events that occurred when MJO-C was active, with values ranging from 0 mm to 900 mm. In Kalimantan, Java, Papua, and parts of the Java Sea, Bali Sea, and Makassar Sea, there has been the most rainfall, ranging from 500 mm to 900 mm. In contrast, the areas of Nusa Tenggara, Maluku, North Maluku, and portions of Sulawesi have rainfall with the lowest values, ranging from 0 mm to 300 mm (Figure 7 (c)).

Interaction of Total Rainfall with MJO-B

One month prior to the 19 September to 19 October 2012 propagation of MJO-B, it was determined that daily rainfall in Indonesia ranged from 0 to 700 mm. The Indian Ocean

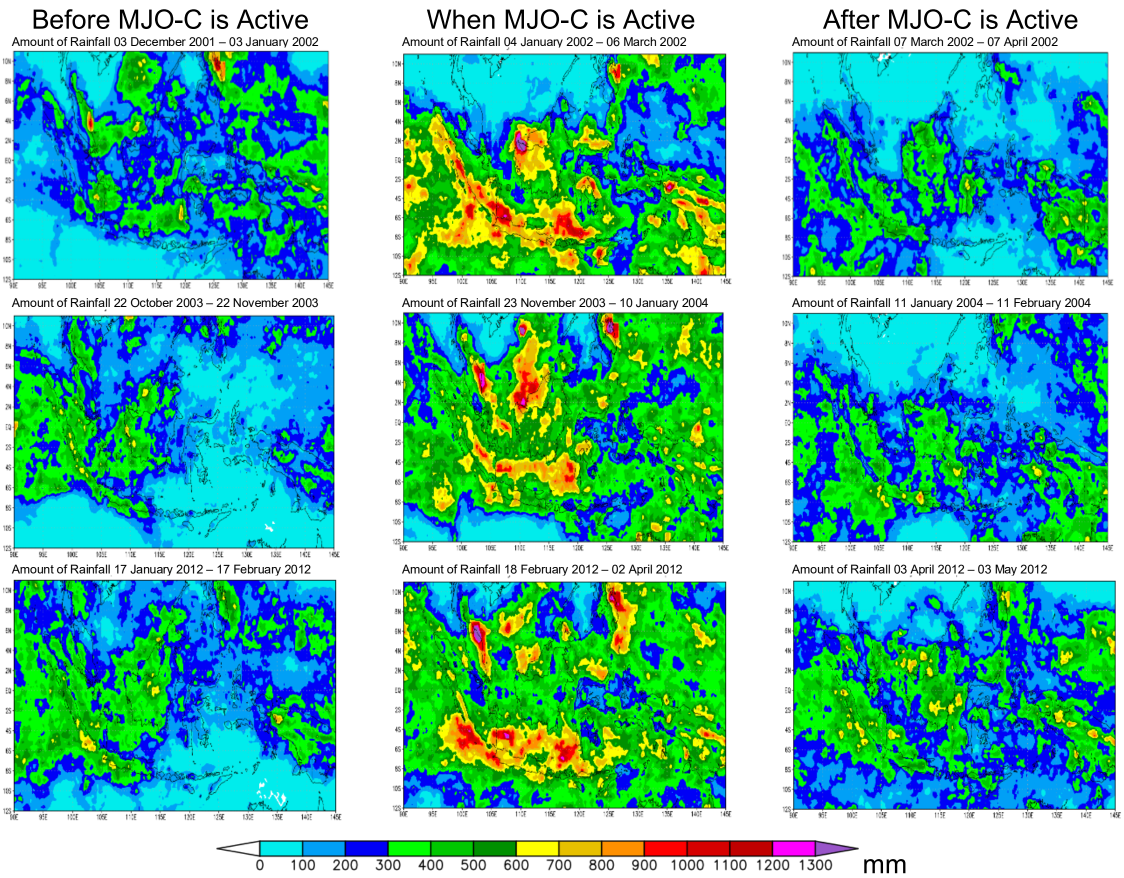

Figure 9. Response of Rainfall Amount to MJO-C Composite (mm)

region west of Sumatra, the island of Sumatra, to Kalimantan receives the greatest amounts of rainfall, with a range of 0 to 700 mm. While the low rainfall amounts, which range from 0 to 300 mm, are dispersed among the areas of Java, Bali, Nusa Tenggara, Maluku, North Maluku, Sulawesi, and Papua (Figure 8 (a)).

The image of the spatial distribution of the amount of rainfall in Indonesian regions from October 20 to November 5, 2012, along with the analysis indicating that most areas in Indonesia did not experience a significant increase or decrease in the amount of rainfall compared to events before MJO-B was active, illustrates the period of MJO-B activity from October 20 to November 5, 2012. The range of rainfall for this time is 0 to 600 millimeters. The Indian Ocean region west of Sumatra and parts of Kalimantan receive the most rainfall with a range of 300 to 600 mm. While the quantity of rainfall with low values is distributed nearly uniformly across Indonesia, notably in Java, Bali, Nusa Tenggara, Maluku, North Maluku, Sulawesi, and Papua, with values ranging from 0 to 200 mm (Figure 8 (b)).

An analysis of the amount of daily rainfall in Indonesia between 0 mm and 1000 mm one month following the MJO-B propagation from November 6 to December 6 of 2012 reveals a range from 0 mm to 1000 mm. The western part of Sumatra, Sumatra Island, Java, and Kalimantan in the Indian Ocean area have the greatest rainfall, which ranges from 600 mm to 1000 mm. While the low rainfall amounts, which range from 0 to 300 mm, are dispersed among the areas of Java, Bali, Nusa Tenggara, Maluku, North Maluku, Sulawesi, and Papua (Figure 8 (c)).

Results of the Effect of MJO Variations of Total Rainfall

Complex atmospheric dynamics in the Indonesian area result in a wide range of rainfall variations. Rainfall variations in Indonesia are impacted by global, regional, and local scale phenomena, including the Asian and Australian monsoons, ENSO, and the Madden Julian Oscillation, on various time frames. The convective effect in the atmosphere has a significant impact on convective cloud formation and precipitation production (Prayuda and Alfuadi, 2015). The production of vast numbers of convective clouds on a big scale is known as Super Cloud Clusters (SCCs), this suggests

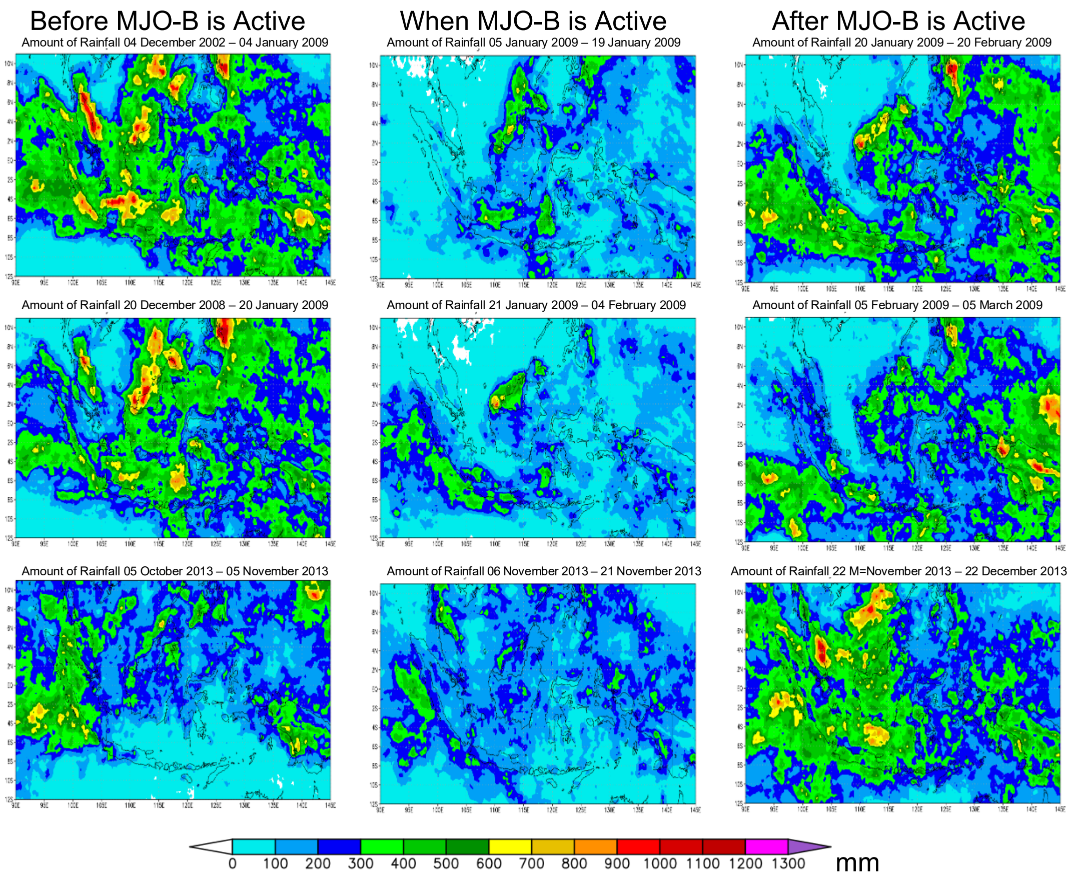

Figure 10. Response of Rainfall Amount to MJO-B Composite (mm)

MJO activity, which might influence rainfall in the Indonesian area (Hermawan, 2010).

This research showed that when MJO-C is active (during MJO-C propagation), there is a greater amount of rainfall than during previous composite occurrences (before and after MJO-C propagation). The increase in rainfall varies over Sumatra, Kalimantan, Java, and a number of regions of Papua Island (Figure 9).

In contrast to the MJO-B event, the reaction of the quantity of rainfall to the MJO-B composite (across millimeters) revealed that the distribution of rainfall in the majority of Indonesia reduced as compared to the composite of previous events (before and after MJO-B propagation) (Figure 10). This is possible because MJO-B was unable to sustain its amplitude, preventing it from crossing 100^o East before weakening and disappearing. This is consistent with the findings of Hidayat's (2016) research, which indicates that the MJO amplitude of the active phase has a significant impact on changes in rainfall and severe rainfall in Indonesia. Rainfall responses to MJO propagation will vary according to the features of distinct regions of Indonesia.

4. Conclusion

MJO-C was able to retain its amplitude after crossing 100° East, while MJO-B was unable to do so and was unable to reach 100° East, weakening till it vanished. This is also based on the spatial outcomes of the Hovmöller diagram for the OLR anomaly. In addition, most parts of Indonesia (Equator to southern hemisphere) witnessed an increase in sea surface temperature in response to the MJO-C and MJO-B events, with a substantial increase during the MJO-C event compared to MJO-B. This is because when the active phase of MJO-C effectively penetrates Indonesia, the activity of the heat flow lost through evaporation reduces, affecting the sea surface temperature.

The increase in sea surface temperature also affects evaporation activity and the production of convective clouds, resulting in an increase in the total of rainfall in Indonesia, particularly towards the equator and the southern hemisphere. Based on the result of this research, it can be said that both MJO-C and MJO-B generally have an impact on the rate of sea surface temperature and rainfall in the Indonesian region, with MJO-C showing a significantly greater reaction than MJO-B.

Further analysis is needed regarding the study of MJO-C and MJO-B in relation to other phenomena that occur in more recent periods, such as their relation to ENSO, and Dipole Mode.

References

Arbain, Ardhi Adhary, F. Renggono, dan R. B. Yahya, 2017, Pengaruh Madden-Julian Oscillation terhadap Distribusi Temporal dan Propagasi Hujan Berdasarkan Pengamatan Radar Cuaca, Jurnal Sains & Teknologi Modifikasi Cuaca, Vol.18, No.2, hal:43-50.

Abdullah, D. 2018. Hubungan Fluktuasi Suhu Permukaan Laut terhadap Kejadian Madden-Julian Oscillation di Kepulauan Nusantara. Skripsi. Makassar: Fakultas Teknik Departemen Teknik Kelautan Universitas Hasanudin Gowa Universitas Hasanuddin Gowa.

Baeda, A. Y., P.'Tonan, C., Abdullah, D. 2019. The correlation between sea surface temperature and MJO incidence in Indonesian waters. In IOP Conference Series: Earth and Environmental Science (Vol. 235, No. 1, p. 012020). IOP Publishing.

Balbeid N., A. S. Atmadipoera, A. F. Koropitan. 2015. Respon Suhu Permukaan Laut (SPL) dan Klorofil-A terhadap Madden Julian Oscillation (MJO) di Laut Indonesia. Jurnal Ilmu dan TeknologiKelautan Tropis, Vol. 7, No. 2, Halaman 553-572.

Bukhari, Wahyu Adi, Kurniawan. 2017. Pendugaan Daerah Penangkapan Ikan Tenggiri Berdasarkan Konsentrasi Distribusi Suhu Permukaan Laut dan Klorofil-a di Perairan Bangka. Jurnal Sumberdaya Perairan. ISSN 1978-1652.

Evana, L., Effendy, S., & Hermawan, E. 2008. Pengembangan Model Prediksi Madden Julian Oscillation (MJO) Berbasis Pada Hasil Analisis Data Real TIME Multivariate Mjo (Rmm1 Dan Rmm2)(Prediction Model Development Madden Julian Oscillation (MJO) Based on the Results of Data Analysis... Agromet, 22(2), 144-159.

Haryanto Y. D.,Yosafat Donni Haryanto, B. Fajar, N. F. Riama, Pengaruh Madden Julian Oscillation (MJO) Terhadap Variabilitas Suhu Permukaan Laut Dan Klorofil-A di Laut Natuna. http://doi.org/10.21107/jk.v14i3.11040

Hidayat, R. (2016). Modulation of Indonesian Rainfall Variability by the Madden-Julian Oscillation. Procedia Environmental

Sciences, 33, 167-177. doi: 10.1016/j.proenv.2016.03.067

Hidayat, R., Kizu, S., 2010, Influence of the Madden-Julian Oscillation on Indonesia Rainfall Variability in Austral Summer, International Journal of Climatology, Vol. 30, hal:1816-1825.

Kerns, B. W., Chen, S. S., 2016, Large-scale precipitation tracking and the MJO over the Maritime Continent and Indo-Pacific warm pool, Journal of Geophysical Research: Atmospheres, vol. 121, pp 8755-8776.

Kim, D., Kim, H., & Lee, M. I. (2017). Why does the MJO detour the Maritime Continent during austral summer. Geophysical Research Letters, 44(5), 2579-2587.

Madden, R. A., dan Julian, P. R., 1972, Description of global-scale circulation cells in the tropics with a 40–50 day period, Journal of The Atmospheri Science, Vol.29, hal:1109 -1123.

Madden, R. A., dan Julian, P. R., 1994, Observations of the 40–50 Day Tropical Oscillation: A review, Mon. Weather Rev, Vol. 112, hal. 814 - 837.

Madden, R., dan Julian, P., 1971, Detection of a 40-50 Day Oscillation in the Zonal Wind in the Tropical Pacific, Journal of The Atmospheric Sciences, Vol. 28, hal:702-708.

Nuryanto, D. M. dan I. U. Badriyah 2014. Pengaruh Perubahan Suhu Permukaan Laut Terhadap Curah Hujan Benua Maritim Indonesia Pada September 2006. Jurnal Meteorologi Dan Geofisika Vol. 15 No. 3 Tahun 2014 : 147-155

Permana, D. S., Thompson, L. G., & Setyadi, G. (2016). Tropical West Pacific moisture dynamics and climate controls on rainfall isotopic ratios in southern Papua, Indonesia. Journal of Geophysical Research: Atmospheres, 121(5), 2222-2245.

Prayuda, S. S., & Alfuadi, N. (2015). Pengaruh Convective Avaliable Potential Energy (CAPE) dan Outgoing Longwave Radiation (OLR) Terhadap Curah Hujan di Cengkareng. In Prosiding Seminar Nasional Fisika dan Aplikasinya.

Seo, H., Subramanian, A.J., Miller, A.J., dan Cavanaugh, N.R., 2014. Coupled

Impacts of the Diurnal Cycle of SPL on the MJO, J. of Clim., 27, 8422-8433. Teknologi Modifikasi Cuaca, Vol.3, No.2, hal.121-124.

Hendon, H.H., C.W. Matthew, and C. Zhang. 2007. Seasonal dependence of the MJO-ENSO relationship. J. Climate, 20:531-543.

Hovmöller E. 1949. The trough-and-ridge diagram. Tellus 1:62–66

Jones C, Waliser DE, Gautier C. 1998. The influence of the Madden–Julian Oscillation on ocean surface heat fluxes and sea surface temperature. J. Climate, 11:1057–1072.

Wirasatriya, A., Prasetyawan, I.B, Triyono, C.D., Muslim & Maslukah, L., 2017. Effect Of ENSO On The Variability Of SST And Chlorophyll-A In Java Sea. 3rd International Conference On Tropical And Coastal Region Buletin Oseanografi Marina Juni 2021 Vol 10 No 2:162–170 170 Studi Persistensi Suhu Permukaan Laut Tinggi (Metrio Swandiko et al.) Eco-Development 2017, IOP Conference Series: Earth and Environmental Science 116:012063

Wirasatriya, A., Prasetyawan, I. B., Triyono, C. D., & Maslukah, L. (2018, February). Effect of ENSO on the variability of SST and Chlorophyll-a in Java Sea. In IOP Conference Series: Earth and Environmental Science (Vol. 116, No. 1, p. 012063). IOP Publishing.

Zhang, C., 2013, Madden-Julian Oscillation Bridging Weather and Climate, American Meteorological Society, hal.1849-1870.

Zhang, C., & Ling, J. (2017). Barrier effect of the Indo-Pacific Maritime Continent on the MJO: Perspectives from tracking MJO precipitation. Journal of Climate, 30(9), 3439-3459.